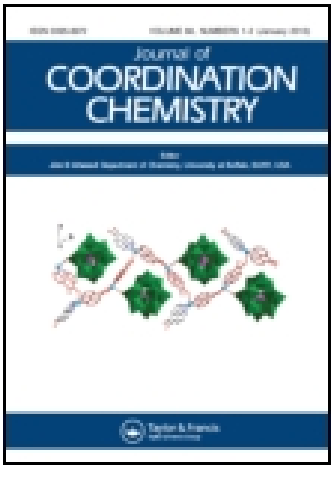

Journal of Coordination Chemistry
Publication details, including instructions for authors and subscription information:
http://www.tandfonline.com/loi/gcoo20

Spectroscopy and theoretical studies of natural melanin (eumelanin) and its complexation by iron(III)

Thiago G. Costa[a], Bruno Szpoganicz[a], Giovanni F. Caramori[b], Vicente R. de Almeida[a], Antônio S. Mangrich[c] & Ana P. Mangoni[c]

[a] Laboratório de Equilíbrio Químico, Departamento de Química, Universidade Federal de Santa Catarina, Florianópolis, Brazil

[b] Grupo de Estrutura Eletrônica Molecular, Departamento de Química, Universidade Federal de Santa Catarina, Florianópolis, Brazil

[c] Laboratório de Química Inorgânica, Universidade Federal do Paraná, Curitiba, Brazil

Accepted author version posted online: 26 Mar 2014.Published online: 14 Apr 2014.

To cite this article: Thiago G. Costa, Bruno Szpoganicz, Giovanni F. Caramori, Vicente R. de Almeida, Antônio S. Mangrich & Ana P. Mangoni (2014) Spectroscopy and theoretical studies of natural melanin (eumelanin) and its complexation by iron(III), Journal of Coordination Chemistry, 67:6, 986-1001, DOI: 10.1080/00958972.2014.905686

To link to this article: http://dx.doi.org/10.1080/00958972.2014.905686

Journal of Coordination Chemistry, 2014
Vol. 67, No. 6, 986–1001, http://dx.doi.org/10.1080/00958972.2014.905686

Spectroscopy and theoretical studies of natural melanin (*eumelanin*) and its complexation by iron(III)

THIAGO G. COSTA†, BRUNO SZPOGANICZ*†, GIOVANNI F. CARAMORI‡, VICENTE R. DE ALMEIDA†, ANTÔNIO S. MANGRICH§ and ANA P. MANGONI§

†Laboratório de Equilíbrio Químico, Departamento de Química, Universidade Federal de Santa Catarina, Florianópolis, Brazil
‡Grupo de Estrutura Eletrônica Molecular, Departamento de Química, Universidade Federal de Santa Catarina, Florianópolis, Brazil
§Laboratório de Química Inorgânica, Universidade Federal do Paraná, Curitiba, Brazil

(*Received 12 November 2013; accepted 14 February 2014*)

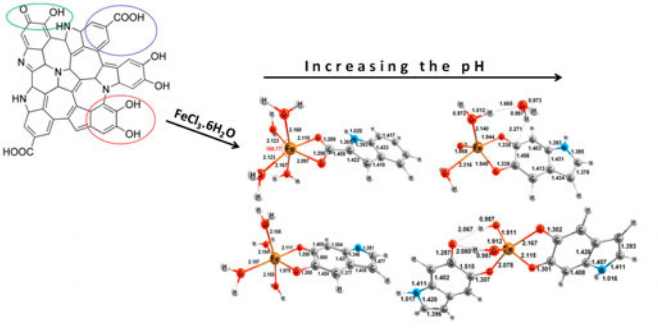

Eumelanin is an oligomeric pigment that has a high affinity for metal ions, which induces the formation of reactive oxygen species, causing melanoma cell apoptosis due to the acceleration of intracellular or extracellular oxidative stress. Melanin in the skin and in dark hair, known as *eumelanin*, has three main groups that serve as donors: carboxylic acid, catechol, and quinone-imine. In this study, *eumelanin* was extracted and purified from dark hair using a modified Prota method and characterized by elemental analysis. The sample shows the absence of sulfur-containing groups, and the infrared spectrum shows characteristic νO–H, νC–H, νC=C, νC=O, and νC–O stretches, which are confirmed by electronic structure calculations. The major interactions with Fe(III) in solution are at acidic pH values: $[Fe(Ac)]^{2+}$ and $[Fe(Qi)]^{2+}$, and at neutral and alkaline pH values: [Fe(OH)(Cat)] and $[Fe(OH)_2(Cat)_2]^{3-}$, evaluated by electronic structure calculations. Electron paramagnetic resonance measurements in the solid state showed that the species isolated at acidic pH provided $g = 4.3$, characteristic for high-spin Fe(III) and the presence of a discrete semi-quinone with $g = 2.003$; at alkaline pH, it was observed that $g = 4.3$, and there was also a large increase in the radical species, suggesting interaction of the metal ion with the catechol.

Keywords: *Eumelanin*; Metal-binding interactions; Fe(III) complexes

*Corresponding author. Email: bruno.s@ufsc.br

1. Introduction

Melanin is a natural pigment obtained from polymerization of the amino acid tyrosine under the action of enzymes. It has received increasing attention [1, 2]. Melanins are molecular aggregates rather than long-chain polymers. Their basic subunits are dihydroxyindole (DHI) and dihydroxyindole-carboxylate (DHICA), which oligomerize to form supramolecular structures containing 3–9 indole units that are assembled in layers, forming aggregates [3]. This oligomer is found in plants, hair, skin (*eumelanins*), and cerebral tissue (*neuromelanins*) of animals [4, 5]. The pigment can be extracted from natural forms or synthesized, usually by auto-oxidation of catechols or by tyrosinase-catalyzed oxidation of tyrosine or dopa. The most widely accepted structure described in the literature is shown in figure 1.

The structure presented in figure 1 shows chelating groups in the oligomers, in particular catechol (Cat) and carboxylic (Ac) groups. Also, there is tautomerization of the quinone-imine (QI) derivative through tautomerization of the DHI subunit. A proposal for this molecular rearrangement is shown in figure 2. These groups are responsible for interaction with metal ions, supported by mass spectroscopy results [5, 6]. The coordination of the above-mentioned groups not only depends on the pH, but also on the characteristics of the metal center [4, 5]. It is believed that ultraviolet rays cause an increase of tyrosinase activity in melanoma cells with melanosomes [4]. This activity is enhanced by the pro-oxidant behavior of the melanin pigment, which is induced by metal ions [7].

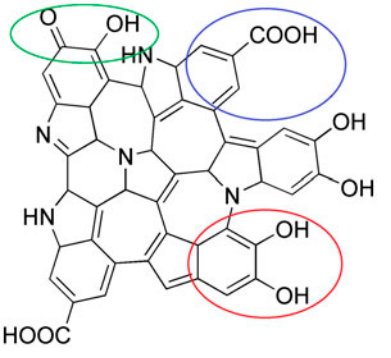

Figure 1. Structure proposed in the literature for natural melanin present in black hair, showing the chelators: carboxylic group in blue circle, catechol group in red circle, and quinone-imine group in green circle (see http://dx.doi.org/10.1080/00958972.2014.905686 for color version).

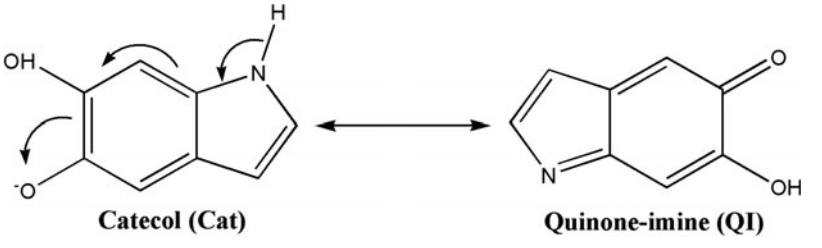

Figure 2. Tautomerization of melanin showing the quinone-imine group formation.

Szpoganicz *et al.* and Gallas *et al.* demonstrated that the affinity of melanin for divalent metal ions has a significant effect on the structure of melanin aggregates [8, 9]. Gallas and coworkers have shown that the metal ions and the acceleration of peroxide bleaching in melanin are related [9]. Furthermore, melanin–copper complexation has been implicated in Fenton-like processes. The same authors also reported that metal ion complexes, which induce passive uptake of the metal ions into cells, show significant anti-melanoma activity [10], confirmed by Farmer and co-authors by the pro-oxidant effects mediated by metals in melanoma cells [11]. These effects can be attributed to Fenton reactions which contribute to the formation of toxic species for melanoma cells like peroxyl, hydroxyl radicals, or singlet dioxygen. Charkoudian and Franz [12] proposed that Fe^{3+} coordination with *neuromelanins* accelerates air oxidation of DHI and DHICA, and refuted the importance of the link between Fe^{3+} and a decrease in Parkinson's disease, resulting from an increase in iron-promoted oxidative stress and malignant neuronal cell death [13–15]. A number of papers have studied the interaction of Fe^{3+} with melanins, but the role of the interaction is not yet understood.

It is well known that synthetic melanin contains only the DHI group, as used by Szpoganicz and co-workers to measure its affinity for Cu^{2+} and Zn^{2+} [8]. On the other hand, the extraction of melanin from natural sources, which is a very complex task, preserves its structural characteristics, allowing a more detailed understanding of its chelating groups and their affinities for metal ions. In this context, the goal of this study was to determine the affinity of *eumelanin*, extracted from hair, for Fe(III). Interactions were characterized by IR and electron paramagnetic resonance (EPR) spectroscopy, by electrochemical methods in order to evaluate the redox active species in the system, and by electronic structure calculations at the density functional theory (DFT) level to determine the structures formed.

2. Materials and methods

2.1. *Natural melanin extraction*

Hair melanin was obtained following the method described by Prota [14] with slight modifications. In summary, black hair was washed with acetone and several times with distilled water to remove any polar contaminants, and then the fat was removed with a few portions of chloroform. (The use of surfactants in this step is not appropriate because it may end up resulting in undesirable residues in the extraction.) After this process, the hair was dried at room temperature and cut into lengths of around 5 cm to increase the contact surface. Approximately, 5 g of hair was homogenized in 50 mL of 0.1 M phosphate buffer, pH 7.5 (this medium is necessary for the enzymatic process), with a glass pestle and submitted to the following treatments: dithiothreitol (0.5 g) was added to the homogenate and the resulting mixture was stirred at 37 °C under a stream of argon for 18 h. Proteinase K (10 mg) and dithiothreitol (0.5 g) were then added to the mixture which was left at 37 °C under argon for an additional 18 h. The mixture was centrifuged for 10 min. The pellet was extensively rinsed with water and then suspended in 30 mL of 0.1 M phosphate buffer, pH 7.5, with papain (10 mg) and dithiothreitol (50 mg). The mixture was stirred for 18 h at 37 °C under argon and centrifuged as described above. The black pellet collected, after six washings with water, was suspended in 10 mL of 0.1 M phosphate buffer, pH 7.5, with protease (10 mg) and dithiothreitol (20 mg). The function of dithiothreitol, proteinase K, and papain

was to hydrolyze the queratin matrix present in the hair. The mixture was then stirred for 18 h at 37 °C under an argon stream. An oxygen-free solution of 2% w/v Triton X-100 was added, and the mixture was stirred for 4 h at room temperature under argon and then centrifuged for 20 min. After washing once with water : methanol 1 : 1 v/v, and four times with water, the black pellet was treated again with protease and dithiothreitol as described above. The pigment pellet, collected by centrifugation, was dried over NaOH overnight and equilibrated with saturated aqueous $CaCl_2$ for 24 h to give 200 mg of melanin.

2.2. *IR spectroscopy*

For IR studies, *eumelanin* was complexed with Fe(III) according to Bilinska's method [16] with slight modifications. This method was used for complexes formed with oligomers and bimolecular systems. Firstly, 50 mg of *eumelanin* was suspended in a 0.5 mM solution of Fe(III) at pH 3.0, 5.0, and 10.0 adjusted using 0.1 M HCl or 0.1 M NaOH solution. In this analysis, $FeCl_3 \cdot 6H_2O$ (Vetec Ltd) was used. After 3 h the mixtures were precipitated at 0 °C and filtered, the pellets were washed with bi-distilled water and dried under vacuum. The analysis was carried out in KBr pellets with approximately 5–10 mg of the sample on a Perkin-Elmer FT-IR 1600 spectrometer with a computerized detection system from 500 to 4000 cm^{-1}.

2.3. *Electrochemistry*

The investigation of the redox species of melanin was performed using cyclic and square-wave voltammetry in a PAR model 273 potentiostat/galvanostat. The experiments were performed in a solution of DMSO under argon atmosphere at room temperature. In this experiment, tetrabutylammonium hexafluorophosphate was used as the supporting electrolyte and an electrolytic cell with three electrodes: working electrode – glassy carbon; auxiliary electrode – platinum; and reference electrode – Ag/Ag^+, calibrated with ferrocene as the internal standard [17].

2.4. *CHNS analysis*

Measurements to determine the percentage of carbon, hydrogen, nitrogen, and sulfur were carried out in a CHNS elemental analyzer – Carlo Erba Model E-1110, at the Central Analytical Chemistry Department – UFSC.

2.5. *EPR measurements*

The EPR spectra of the solutions in a 2 : 1 M ratio of melanin : iron at pH 3 and 10 were obtained at 77 K on a Bruker EMX spectrophotometer operating in the X band mode (~9.5 GHz) using a 100 kHz modulation frequency and 0.05 mT amplitude modulation. The samples were firmly accommodated in quartz tubes of 3 mm internal diameter. The parameter values were obtained by treatment of the experimental spectra with the aid of WinEPR software (Bruker).

2.6. *Theoretical methods*

The electronic structure calculations for ligands and iron(III) complexes, including geometry optimizations and stretching frequencies, were performed employing DFT, with the Becke [18] correlation and Perdew exchange functional [19], BP86 [20], in conjunction with the Ahlrichs TZVP basis set [21]. The calculations were performed using the Gaussian 03 [22] and ORCA 2.7.0 [23] software applications.

3. Results and discussion

3.1. *Characterization of* eumelanin *extracted from hair*

3.1.1. CHNS analysis. One feature of the *eumelanins* that differs markedly from the *pheomelanin* is the absence of sulfur groups. After the first extraction using only one washing with dithiothreitol, the elemental analysis revealed the presence of sulfur. These groups are assigned by Prota and coworkers [14] as possible natural contaminants present in the hair sample and even cysteinyl groups from some types of hair melanogenesis. After four washes of the pigment with dithiothreitol, the absence of sulfur groups was observed. The elemental analysis results indicated C 70.12%, H 3.88%, N 8.90%, and O 17.10%. Similar results are found in the literature for pure *eumelanins* [8, 10, 12]. It is worth remembering that the purity of the pigment after the extraction ranges from hair to hair, and according to the experimental conditions.

3.1.2. Electrochemistry. The cyclic voltammogram of pure *eumelanin* is shown in figure 3. An irreversible wave was observed at $E_{pc} = 0.06$ V, characteristic of the reduction of quinone groups present in the biomolecule to semiquinone. When a more cathodic potential was used, the peak was classified as quasi-reversible with $E_{1/2} = -0.47$ V, representing the semiquinone/catechol redox couple, electrochemically generated from the reduction of semiquinone groups previously present in the solution. Both redox processes occur with electron transfer governed by diffusion.

The square wave voltammogram shown in figure 4 verifies that the redox process previously evidenced by cyclic voltammetry occurs in melanins [9]. The wave characteristic of the reduction of semiquinone is asymmetric, attributed to the fact that rather than containing one uniform oligomer, the type and quantity of monomers in the *eumelanin* structure are variable. Other authors have shown that melanins are not polymers of high-molecular-weight oligomers but instead have measurable numbers of monomers. The structures involved in the redox processes associated with *eumelanins* are shown in figure 5.

3.1.3. IR spectroscopy. Structures of the three main donor groups present in *eumelanin* (catechol, quinone-imine, and carboxylate) were optimized and then employed to estimate theoretical IR spectra, revealing that all groups have a planar geometry (figure 6). The theoretical IR spectra for these *eumelanin* groups are shown in figure 7. The spectrum for the quinone-imine shows a band characteristic of νO–H at 3666 cm^{-1}, followed by two small peaks at 3052 and 3088 cm^{-1}, respectively, related to the νC–H of the indole ring present in the group. This stretch was also evident in the experimental spectrum at 1605 and 1532 cm^{-1},

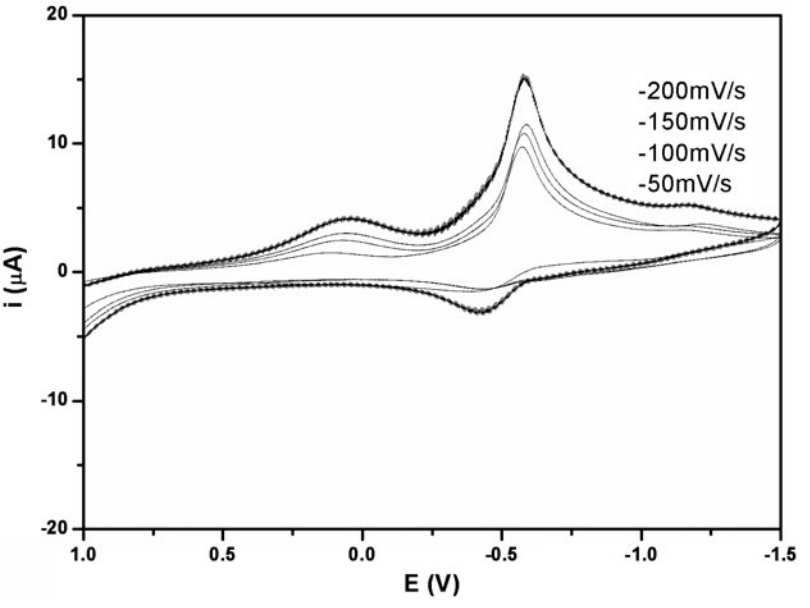

Figure 3. Cyclic voltammogram of a 0.0001 M solution of *eumelanin* in DMSO, with scan rates of 200, 150, 100, and 50 mV s^{-1} at 25 °C. Supporting electrolyte: 0.1 M TBAP; Electrodes: working glassy carbon, reference: Ag/Ag^{+}, counter electrode: Pt wire; internal standard Fc/Fc^{+}.

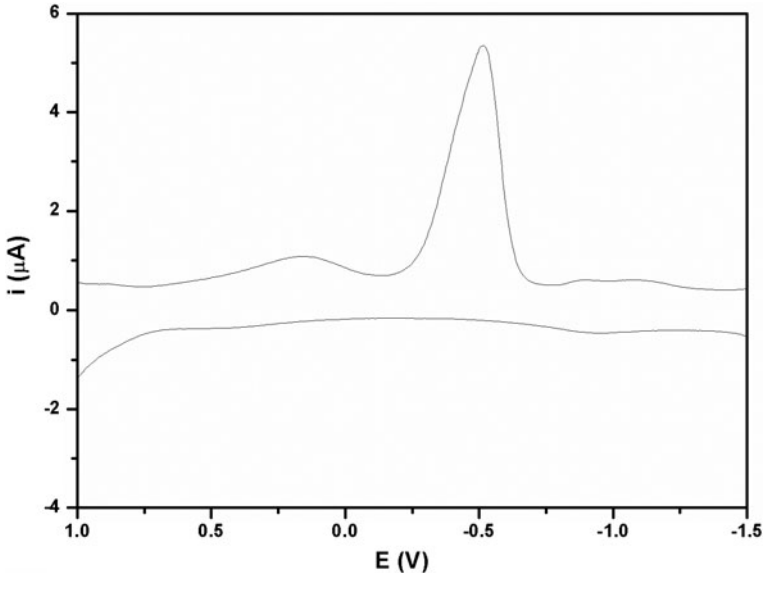

Figure 4. Square wave voltammogram of a 0.0001 M solution of *eumelanin* at 25 °C. Supporting electrolyte 0.1 M TBAP; Electrodes: working glassy carbon, reference: Ag/Ag^{+}, counter electrode: Pt wire; internal standard Fc/Fc^{+}.

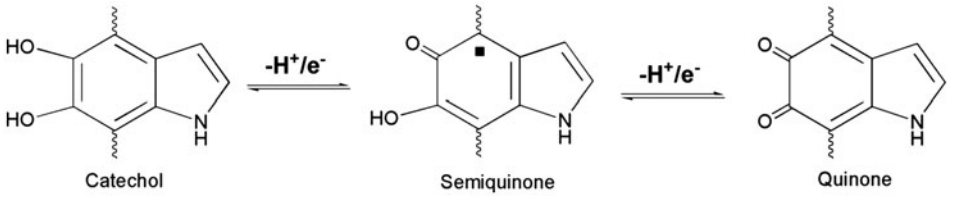

Figure 5. Schematic structures involved in redox processes associated with *eumelanin*, showing the oxidation of catechol to quinone, passing through an intermediate semi-quinone radical.

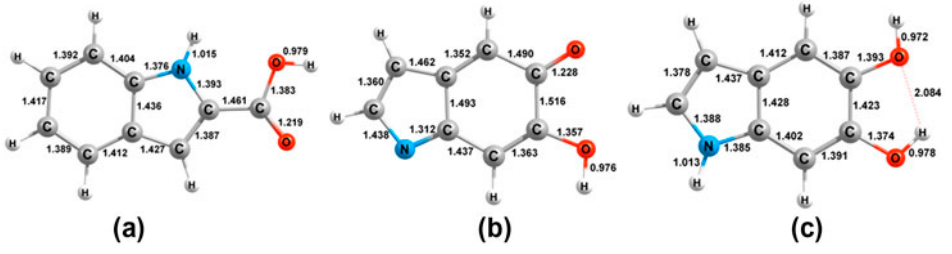

Figure 6. Optimized geometries of (a) carboxylic group, (b) quinone-imine, and (c) catechol ligands, obtained by BP86/TZVP level of theory.

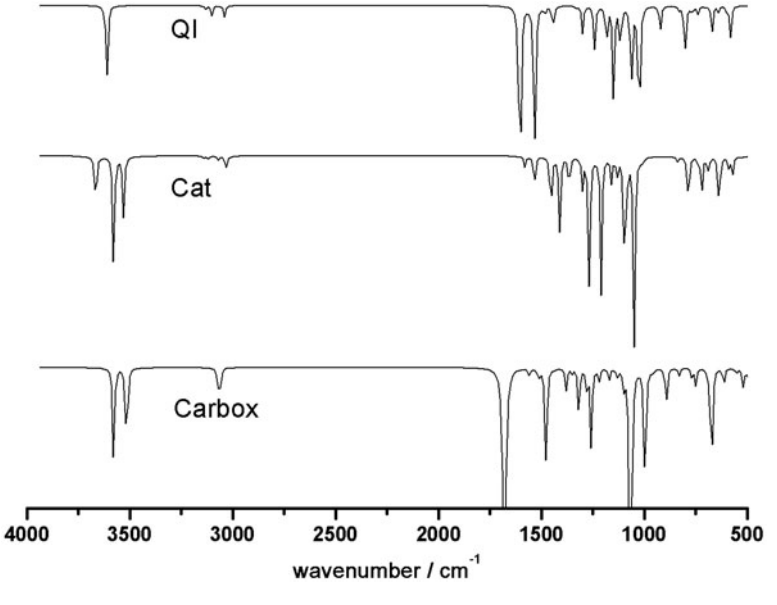

Figure 7. Simulated IR spectra for the structures optimized computationally, showing the characteristic stretch of each group present in natural *eumelanin*.

Table 1. Summary of the major theoretical and experimental stretching frequencies correlating the main bands observed for melanin.

Ligand	Vibration type (ν)	Theoretical (cm^{-1})	Experimental (cm^{-1})
Ac	(C=C)	–	
	(C–O)	1070	1051
	(C=O)	1614	1530–1688 (large)
QI	(C=C)	1532	1530–1688 (large)
	(C–O)	1022	1051
	(C=O)	1605	1530–1688 (large)
Cat	(C=C)	1532	1530–1688 (large)
	(C–O)	1052	1051

representing the νC=C and νC=O, respectively. These vibrations fall within the region observed in the experimental spectrum for these groups. For the last band of importance, a νC–O at 1051 cm^{-1} was also observed in the experimental spectrum.

The theoretical spectrum for catechol shows a band characteristic of νO–H for the molecule. Again we see a stretch at 3000 cm^{-1} for νC–H present in the indole ring and νC=C of the rings present in the molecule at 1532 cm^{-1}. With the absence of a carbonyl in this ligand there is a small contribution from the catechol to this region of the spectrum. Thus, we can associate the broad band at 1530–1688 cm^{-1} mainly with νC=O present in the carboxylic and quinone-imine groups. Finally, we noted that the band at 1052 cm^{-1} from νC–O was evidenced for this ligand.

The last group simulated was the carboxylic, which presents νO–H at 3583 cm^{-1}. It also exhibits a weak νC–H at 3020 cm^{-1}, corresponding to the indole ring, as observed for the other two groups. A high intensity band was present at 1681 cm^{-1}, corresponding to νC=O. In the simulated spectra for the carboxylic and quinone-imine groups, there is an increase in the νC=O stretching for the carboxylic in comparison with the quinone-imine group. The νC–O of the carboxylic group at 1052 cm^{-1} was also confirmed in the experimental spectrum. The experimental IR spectrum for *eumelanin* extracted from hair (*free eumelanin*) reveals a broad band between 1530 and 1688 cm^{-1}, which is related to νC=C coupled vibrations present in the rings of the bio-conjugated oligomers in both donor groups. The experimental spectra also reveal the presence of νC=O of carboxylic and quinone-imine. There is also a band at 1051 cm^{-1} related to νC–O, present in carboxylic, catechol, and quinone-imine groups. The intensity of this band is quite low due to the presence of carbonyl groups. Table 1 shows a summary of the comparisons between the theoretical and experimental IR spectroscopy studies correlating the intensity of the main bands in the system.

3.2. *Characterization of eumelanin interaction with Fe(III) ion*

Equilibrium constants associated with the interactions of the Fe(III)-*eumelanin* system were determined by potentiometric titration [24]. The major interactions detected by Szpoganicz *et al.* are shown in figure 8. At biological pH, the major interaction is [Fe(Cat)(OH)] which can be correlated with the mechanism of *eumelanin* formation. Leonard and coworkers [15] reported the influence of metal ions on the dopachrome conversion in melanin at this pH. This may involve oxidation of catechol groups present in the precursors of *eumelanin* under certain conditions, thus increasing the efficiency of oligomer formation. A recent report shows the influence of vanadium haloperoxidase enzymes in the formation of synthetic

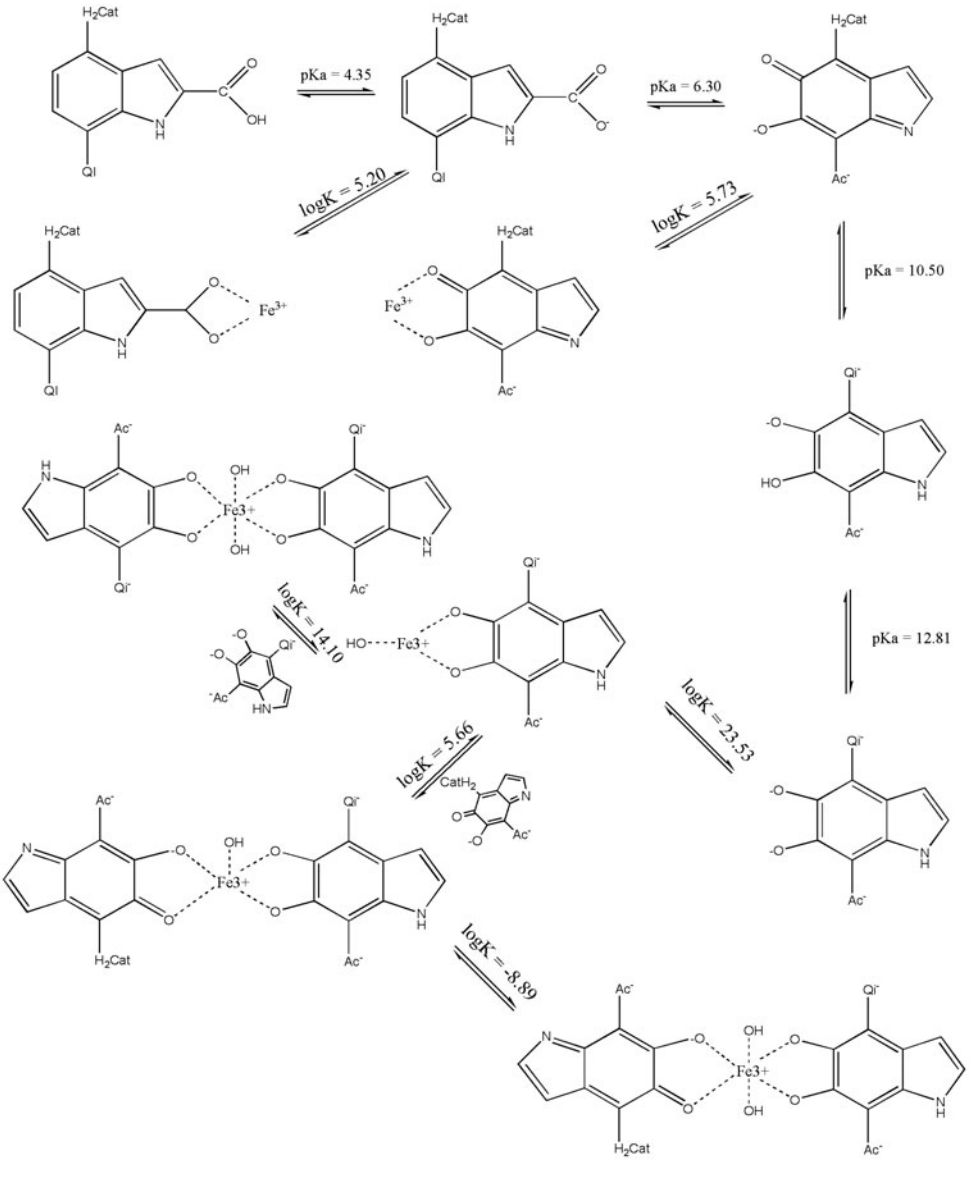

Figure 8. Major equilibria detected by potentiometric titration taken from Ref. [24].

melanins [25]. Also, the metal center plays a role in melanin formation at this pH due to interaction with catechol groups.

Korytowski studied the reactive species produced upon irradiation of melanin with UV and visible light [26]. In the presence of EDTA, the production of reactive oxygen species increased for melanin complexed with iron. To explain their results, they proposed that melanin first reduces Fe(III) to Fe(II), followed by extraction of Fe(II) by EDTA. Both EDTA-Fe(II) and melanin-Fe(II) can catalyze the Fenton reaction, thereby increasing the

production of free radicals. This study once again highlights the importance of elucidating the distribution of oxidation states of the bound iron.

The major species will be the starting point for spectroscopic studies and theoretical calculations.

3.2.1. Electronic structure calculations. In order to obtain information on the structures of the complexes obtained, theoretical calculations were performed for a set of complexes based on the species distributions (figure 8) and considering the major species formed at acidic, neutral, and alkaline pH. Geometry optimizations at the BP86/TZVP level were performed considering octahedral geometries as the starting point (since these iron complexes have O-donors), in which the free coordination site is occupied by water, in order to simulate the species found in solution. For instance, for the $[Fe(Ac)]^{2+}$ interaction, four waters were used as ligands to achieve an octahedral structure $[Fe(Ac)(H_2O)_4]^{2+}$ [figure 9(a)]. In this case, the optimized structure converges to distorted octahedral. A similar procedure was adopted for $[Fe(Qi)]^{2+}$ which, after the geometry optimization, provided a similar distorted octahedral structure $[Fe(Qi)(H_2O)_4]^{2+}$ [figure 9(b)]. These two structures are very similar, despite the intrinsic structural differences between Ac^- and Qi^-, as shown in Section 3.1.3. For [Fe(OH)(Cat)], octahedral starting geometries including three water molecules and a hydroxide as ligands were also considered, $[Fe(OH)(Cat)(H_2O)_3]$, in which the hydroxide was placed along three different vertices of the octahedron, two in the equatorial (x–y) plane and one on the (z) apical axis (see figure S1 – Supplementary material, see online supplemental material at http://dx.doi.org/10.1080/00958972.2014.905686). A remarkable feature of the $[Fe(OH)(Cat)(H_2O)_3]$ structures is that they all converge to a final distorted trigonal-bipyramidal geometry, in which hydroxide remains coordinated and one water migrates to form hydrogen bonds at different positions, as shown in figure 9(c)–(e). According to figure 9(c)–(e), the water molecule forms hydrogen bonds not only by interacting with coordinated hydroxide [figure 9(c)] but also binding with water [figure 9(d)] and the coordinated oxygen of the catecholate [figure 9(e)]. All optimized structures for $[Fe(OH)(Cat)(H_2O)_3]$ are very similar in terms of energy stability, which is attributed to the small energy barrier connecting the local minima on the potential energy surface. For $[Fe(OH)_2(Cat)_2]^{3-}$, an initial octahedral structure was considered. However, after the geometry convergence, a distorted trigonal-bipyramidal geometry was obtained, in which both hydroxides form intramolecular hydrogen bonds with oxygen from a catechol group, as shown in figure 9(f).

3.2.2. IR spectroscopy. Experimental infrared spectra of the isolated complexes at pH 3, 5, and 10 are shown in figure 10. The free *eumelanin* spectrum shows a broad band with a minimum at 1664 cm^{-1} which is attributed to the overlapping of these three major groups (Cat, QI, and Ac); their respective shifts in the presence of Fe(III) are discussed below. At pH 3, the predominant species are $[Fe(Qi)]^{2+}$ and $[Fe(Ac)]^{2+}$ in the solid complex and we observe a shift of 60 cm^{-1} in νC=O band after coordination of this group to the Fe(III), demonstrating coordination of quinone-imine and acetate. There was also a shift of 8 cm^{-1} in νC–O, characterizing the interaction of these groups. At pH 5 the major interaction is [Fe(Cat)(OH)], and at lower pH a shift in the characteristic stretch of C=C and C=O of 17 cm^{-1} was observed in the isolated spectrum, indicating a possible coordination to catechol, since the change in νC–O remained fairly constant at 15 cm^{-1}. In comparison, at pH 3 phenolic groups coordinate to the metal. At pH 10, variation in νC=C and νC=O shifts is

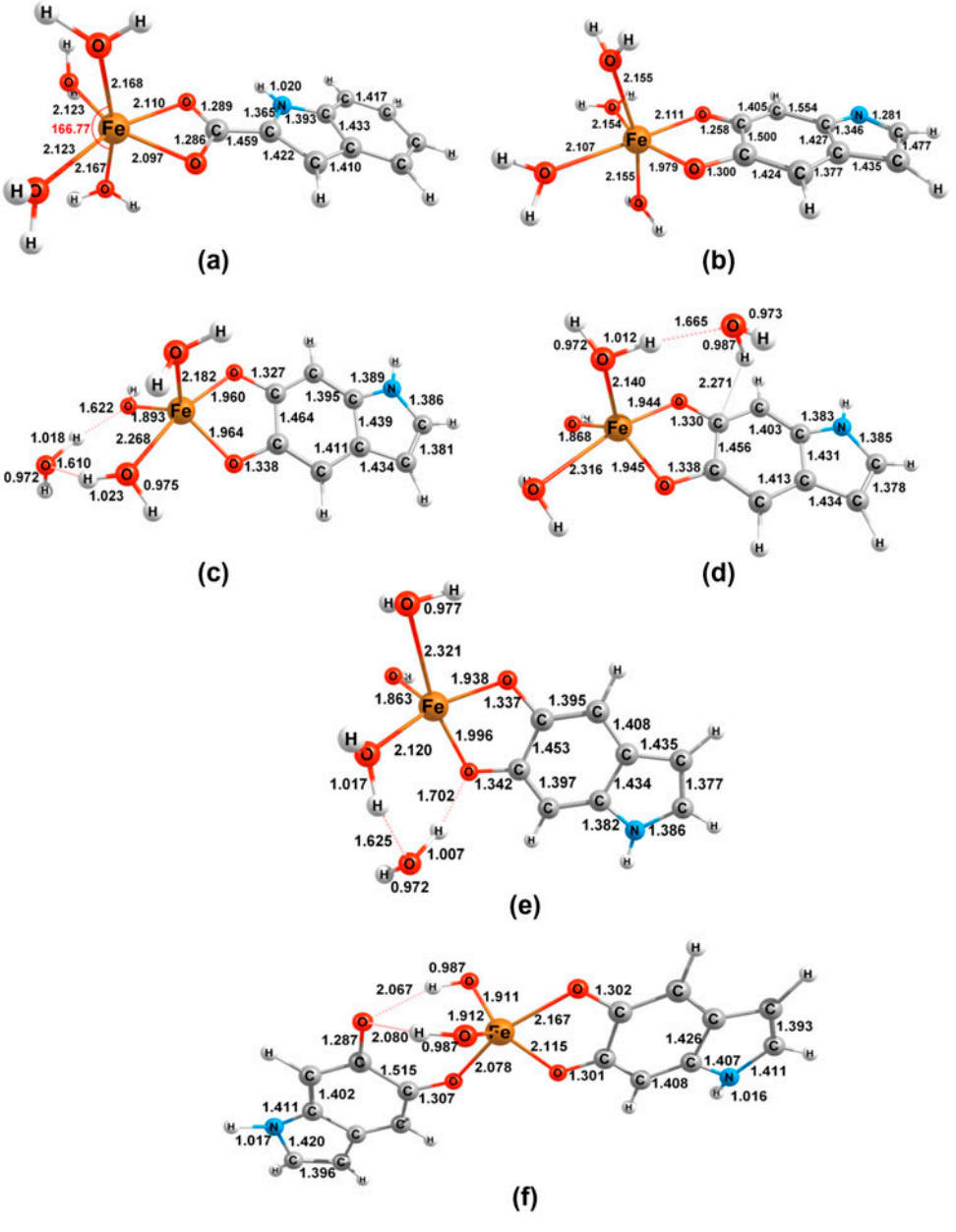

Figure 9. Optimized geometries of (a) $[Fe(Ac)(H_2O)_4]^{2+}$, (b) $[Fe(Qi)(H_2O)_4]^{2+}$, (c)–(e) $[Fe(OH)(Cat)(H_2O)_3]$, and (f) $[Fe(OH)_2(Cat)_2]^{3-}$.

25 cm^{-1}. The major species at this pH are $[Fe(Cat)_2(OH)_2]^{3-}$ and $[Fe(Cat)(Qi)(OH)_2]^{2-}$. In comparison with pH 5, the shift is greater due to contribution of the shift associated with coordination of the quinone-imine groups. Shurygina and coworkers [27] identified the same shifts in this region associated with coordination of divalent groups like Cu(II) and

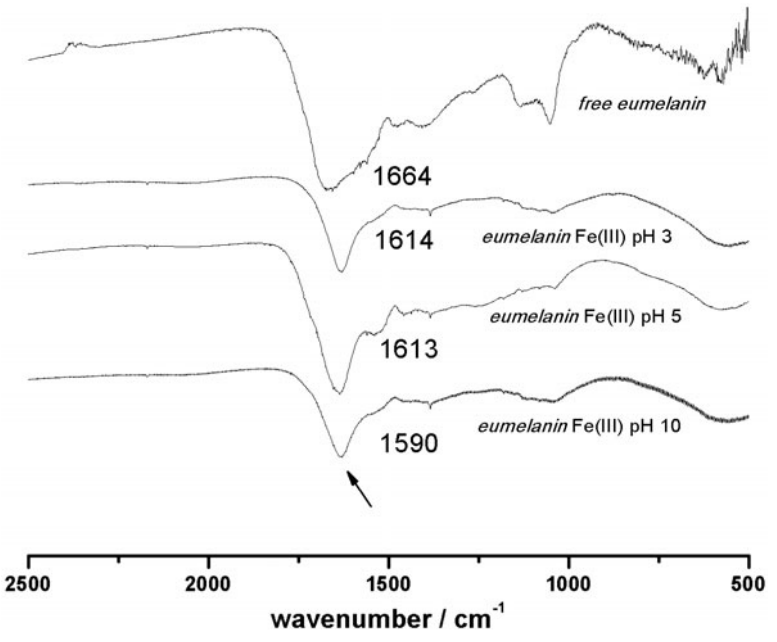

Figure 10. IR spectrum showing the stretch for free melanin from hair and in the presence of Fe(III) in a 2 : 1 *eumelanin* : metal ratio at pH 3, 7, and 10.

Zn(II). However, the shifts observed in our study were higher, due to the strength of the metal center and the interaction under study [26, 27]. Comparing infrared spectra of the above-mentioned species in solution and in the solid state, a good correlation was found, indicating that both donor groups are present in these media.

The simulated IR spectra for the major interactions in the *eumelanin* : Fe(III) system are shown in figure 11. These were obtained through determination of the Hessian matrix eigenvalues at the BP86/TZVP level, employing the optimized structures listed in figure 11. In the theoretical spectrum of $[Fe(QI)]^{2+}$ and $[Fe(Ac)]^{2+}$, νC=C and νC=O coupled stretches were observed at 1530 and 1540 cm^{-1}, respectively, which represent shifts of 64 and 74 cm^{-1} related to the free ligand, respectively. Shifts of 11 and 18 cm^{-1} corresponding to νC–O indicate coordination of this group, resembling the shift observed in the experimental spectrum, showing the formation of these species in the pH range studied. Since νC=C and νC–O stretches of [Fe(Cat)(OH)] are found at 1572 and 1118 cm^{-1}, respectively, there is only a slight shift in relation to the previous species, which indicates coordination to the catecholate and confirms the data obtained experimentally. According to simulated spectra, the shifts in νC=C and νC–O of $[Fe(Cat)_2(OH)_2]^{3-}$ are larger and smaller, respectively, than those of [Fe(Cat)(OH)], confirming a 2 : 1 catechol : Fe(III) ratio. These shifts at 1500 and 1016 cm^{-1} show the interaction between the chelating groups present in melanin and the metal center, as previously observed in the experimental study. A summary of the principal shifts observed are shown in table 2. Simon and Hong [28] studied the interactions between Sepia *eumelanins* and divalent cations, and an energy decrease related to νC=O and νOH groups due to complexation with the metal center was observed. In our work, a similar decrease was also evident.

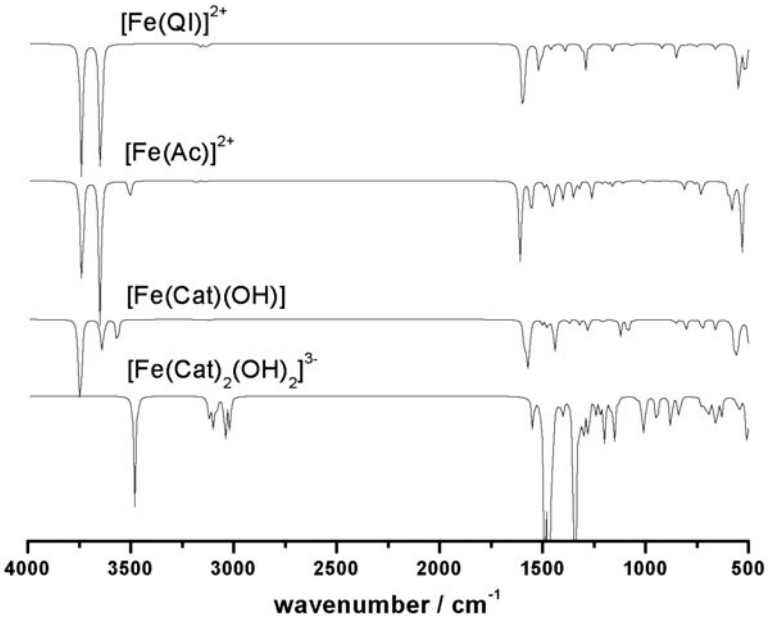

Figure 11. Simulated IR spectra for the main interactions in the *eumelanin*: Fe(III) system, optimized computationally at each pH identified in the potentiometric titration.

Table 2. Summary of the major stretches observed for the *eumelanin*-Fe(III) system and the corresponding theoretical and experimental shifts showing the interaction of the main donors with iron(III).

Species	pH	Vibration type (ν)	Theoretical $\nu/\Delta\nu$ (cm^{-1})	Experimental $\Delta\nu$ (cm^{-1})
$[Fe(Qi)]^{2-}$	3	(C=C) (C=O)	1541/64	60
		(C–O)	1006/16	8
$[Fe(Ac)]^{2-}$		(C=C) (C=O)	1540/74	60
		(C–O)	1059/11	8
[Fe(Cat)(OH)]	5	(C=C)	1512/20	17
		(C–O)	1037/15	12
$[Fe(Cat)_2(OH)_2]^{3-}$	10	(C=C)	1503/29	25
		(C–O)	1032/20	16

3.2.3. Electron paramagnetic resonance. The EPR spectra of *eumelanin* complexed to Fe(III) at pH 3 and 10 are shown in figure 12. At pH 3 there is a signal at $g = 4.3$ (1500 G) of Fe(III), occupying either tetrahedral or octahedral rhombic distorted site. There is also a discrete signal at $g = 2.003$ for an electron, in this case a semi-quinone radical species. This species was also observed in the electrochemistry and supports the proposed melanin structure with the formation of radical species [29–31]. The EPR spectrum at pH 10 reveals a signal at $g = 4.3$, characteristic of high-spin Fe(III) but with a different coordination environment, bound to the catechol groups. The signal characteristic of the radical species shows a significant increase in the presence of iron, favoring the formation of semiquinones, thus indicating interaction between catechol and Fe(III) at pH 10. Barreto and coworkers [32], in studies on the interaction of metals with dioxylene ligands, observed a

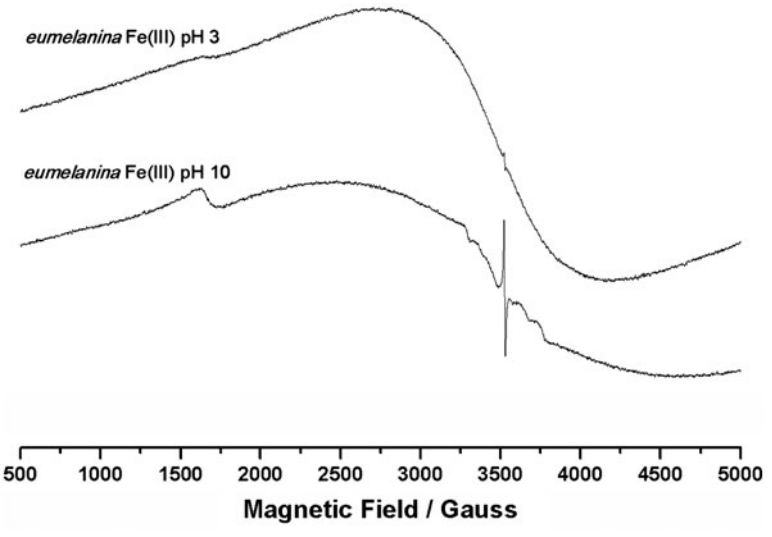

Figure 12. EPR spectra for *eumelanin*-Fe(III) isolated at pH 3 and 10 in a 2 : 1 M ratio of melanin : iron at pH 4 and 10 obtained at 77 K.

similar spectrum, with both signals showing interactions of divalent and trivalent metals by these groups. The interactions at pH 3 observed from the EPR results, supported by the IR spectroscopic analysis, and potentiometric titration can be attributed to coordination of the carboxylic and quinone-imine groups. The EPR spectra also depict broad lines, $g \approx 2.2$ (2500–4500 G) typical of Fe(III) ion clusters. The greater line width at pH 10 means that the Fe(III) cluster increased at higher pH perhaps from oxidation of some Fe(II) ions existing on the material.

4. Conclusion

This study investigated the functional groups present in natural *eumelanins* extracted from hair by elemental analysis, infrared spectroscopy, and theoretical calculations of sub-units of melanin. Redox processes occurring in the oligomer were evidenced by cyclic and square wave voltammetry, confirming the presence of the three main groups, carboxylic acid, catechol, and quinone-imine. The oligomer exhibits a strong affinity for Fe(III), as shown previously. At acidic pH, the interaction of the oligomer with iron(III) occurs through quinone-imine and carboxylic groups. At near neutral pH values, the interaction occurs mainly via the catechol. However, on increasing the pH values to over 6, there is formation of mixed species in a 2 : 1 catechol : quinone-imine ratio. For higher pH values, such as 8, the predominant interaction occurs in a 2 : 1 catechol : iron(III) ratio. The major species, representing the aqua complexes, were optimized through electronic structure calculations at the DFT level of theory. Infrared spectroscopy revealed the main functional groups present in melanin in the solid state, and also indicated the interaction between *eumelanin* and iron (III). EPR spectroscopy enabled the identification of the species present at pH 3 and 10 and showed characteristic *g* values for iron(III) in different coordination environments.

The results of this study helped to elucidate some properties of melanins, such as their interaction with iron(III), for which iron(III) has to be liberated in order to bind to melanin. These findings can aid the synthesis of Fe(III) complexes that could be tested for anti-melanoma properties.

Supplementary material

A picture showing the starting octahedral geometries for the [Fe(OH)(Cat)] species, including three water molecules and an hydroxide ion as ligands, is available free of charge at http://www.tandfonline.com/toc/gcoo20/current#.Uz1JLahdXcA.

Funding

This study was financially supported by the Brazilian government agency CNPq (Conselho Nacional de Pesquisa e Tecnologia) and the infrastructure was provided by UFSC (Universidade Federal de Santa Catarina). G.F. Caramori is grateful to the Santa Catarina state government agency FAPESC for financial support through [grant number 17.413/2009-0] and also to CENAPAD/SP for access to computational facilities.

References

[1] R.A. Gortner. *J. Biol. Chem.*, **8**, 341 (1910).
[2] W. Young. *J. Biol. Chem.*, **8**, 460 (1920).
[3] R.A. Nicolaus. *Melanins*, Vol. 3, pp. 100–199, Hermann, Paris, (1968).
[4] G. Prota. *Melanins and Melanogenesis*., Academic Press, San Diego, CA (1992).
[5] A. Dzierzega-Lecznar, S. Kurkiewicz, K. Stepien, E. Chodurek, P. Riederer, M. Gerlach. *J. Neural Transm.*, **113**, 729 (2006).
[6] H.Z. Hill. *BioEssays*, **14**, 49 (1992).
[7] E.V. Gan, H.F. Haberman, I.A. Menon. *Biochim. Biophys. Acta*, **370**, 62 (1974).
[8] B. Szpoganicz, S. Gidanian, P. Kong, P. Farmer. *J. Inorg. Biochem.*, **89**, 45 (2002).
[9] J.M. Gallas, K.C. Littrell, S. Seifert, G.W. Zajac, P. Thiyagarajan. *Biophys. J.*, **77**, 1135 (1999).
[10] D. Cen, D. Brayton, B. Shahandeh, F.L. Meyskens, Jr, P.J. Farmer. *J. Med. Chem.*, **47**, 6914 (2004).
[11] P.J. Farmer, S. Gidanian, B. Shahandeh, A.J. Di Bilio, N. Tohidian, F.L. Meyskens, Jr. *Pigm. Cell Res.*, **16**, 273 (2003).
[12] L.K. Charkoudian, K.J. Franz. *Inorg. Chem.*, **45**, 3657 (2006).
[13] L. Zecca, M.B.H. Youdim, P. Riederer, J.R. Connor, R.R. Crichton. *Nature Rev. Neurosci.*, **5**, 863 (2004).
[14] L. Novellino, A. Napolitano, G. Prota. *Biochim. Biophys. Acta*, **1475**, 295 (2000).
[15] L.J. Leonard, D. Townsend, R.A. King. *Biochemistry*, **27**, 6156 (1988).
[16] B. Bilińska. *Spectrochim. Acta Part A*, **57**, 2525 (2001).
[17] R.R. Gagne, C.A. Koval, G.C. Lisensky. *Inorg. Chem.*, **19**, 2854 (1980).
[18] A.D. Becke. *Phys. Rev. A*, **38**, 3098 (1988).
[19] J.P. Perdew. *Phys. Rev. B*, **34**, 7406 (1986).
[20] J.P. Perdew, W. Yue. *Phys. Rev. B*, **33**, 8800 (1986).
[21] F. Weigend, R. Ahlrichs. *Phys. Chem. Chem. Phys.*, **7**, 3297 (2005).
[22] M.J. Frisch, G.W. Trucks, H.B. Schlegel, G.E. Scuseria, M.A. Robb, J.R. Cheeseman, J.A. Montgomery, Jr., T. Vreven, K.N. Kudin, J.C. Burant, J.M. Millam, S.S. Iyengar, J. Tomasi, V. Barone, B. Mennucci, M. Cossi, G. Scalmani, N. Rega, G.A. Petersson, H. Nakatsuji, M. Hada, M. Ehara, K. Toyota, R. Fukuda, J. Hasegawa, M. Ishida, T. Nakajima, Y. Honda, O. Kitao, H. Nakai, M. Klene, X. Li, J.E. Knox, H.P. Hratchian, J.B. Cross, V. Bakken, C. Adamo, J. Jaramillo, R. Gomperts, R.E. Stratmann, O. Yazyev, A.J. Austin, R. Cammi, C. Pomelli, J.W. Ochterski, P.Y. Ayala, K. Morokuma, G.A. Voth, P. Salvador, J.J. Dannenberg, V.G. Zakrzewski, S. Dapprich, A.D. Daniels, M.C. Strain, O. Farkas, D.K. Malick, A.D. Rabuck, K. Raghavachari, J.B. Foresman, J.V. Ortiz, Q. Cui, A.G. Baboul, S. Clifford, J. Cioslowski, B.B. Stefanov, G. Liu, A. Liashenko, P. Piskorz, I. Komaromi, R.L. Martin, D.J. Fox, T. Keith, M.A. Al-Laham, C.Y. Peng,

A. Nanayakkara, M. Challacombe, P.M.W. Gill, B. Johnson, W. Chen, M.W. Wong, C. Gonzalez, J.A. Pople. *Gaussian 03, Revision D.01*, Gaussian, Inc., Wallingford, CT (2004).
[23] F. Neese. *Coord. Chem. Rev.*, **253**, 526 (2009).
[24] T.G. Costa, R. Younger, C. Poe, P.J. Farmer, B. Szpoganicz. *Bioinorg. Chem. Appl.*, **2012**, 9 (2012). doi:10.1155/2012/712840.
[25] M. Nicolai, G. Gonçalves, F. Natalio, M. Humanes. *J. Inorg. Biochem.*, **105**, 887 (2011).
[26] W. Korytowski, B. Pilas, T. Sarna, B. Kalyanaraman. *Photochem. Photobiol.*, **45**, 185 (1987).
[27] E.A. Shurygina, N.K. Larina, M.A. Chubarova, M.M. Kononova. *Geoderma*, **6**, 169 (1971).
[28] J.D. Simon, L. Hong. *Photochem. Photobiol.*, **82**, 1265 (2006).
[29] K. Nakamoto, Y. Morimoto, A.E. Martell. *J. Am. Chem. Soc.*, **83**, 4528 (1961).
[30] J.B. Nofsinger, S.E. Forest, L.M. Eibest, K.A. Gold, J.D. Simon. *Pigm. Cell Res.*, **13**, 179 (2000).
[31] L. Mosca, C. De Marco, M. Fontana, M.A. Rosei. *Arch. Biochem. Biophys.*, **371**, 63 (1999).
[32] W.J. Barreto, R.A. Ando, P.S. Santos, W.P. Silva. *Spectrochim. Acta, Part A*, **68**, 612 (2007).